European Journal of Medicinal Chemistry 224 (2021) 113736

Contents lists available at ScienceDirect

European Journal of Medicinal Chemistry

journal homepage: http://www.elsevier.com/locate/ejmech

Enhanced pyrazolopyrimidinones cytotoxicity against glioblastoma cells activated by ROS-Generating cold atmospheric plasma

Zhonglei He [a, b, c, d, *], Clara Charleton [e], Robert W. Devine [e], Mark Kelada [e], John M.D. Walsh [e], Gillian E. Conway [a, c, f], Sebnem Gunes [a, c], Julie Rose Mae Mondala [a, c], Furong Tian [a, b, c], Brijesh Tiwari [g], Gemma K. Kinsella [a, c], Renee Malone [a, c], Denis O'Shea [a, c], Michael Devereux [a, c], Wenxin Wang [d], Patrick J. Cullen [h], John C. Stephens [e, i], James F. Curtin [a, b, c, *]

[a] BioPlasma Research Group, School of Food Science and Environmental Health, Technological University Dublin, Dublin, Ireland
[b] Nanolab, FOCAS Research Institute, Technological University Dublin, Dublin, Ireland
[c] Environmental, Sustainability and Health Research Institute, Technological University Dublin, Dublin, Ireland
[d] Charles Institute of Dermatology, School of Medicine, University College Dublin, Dublin, Ireland
[e] Department of Chemistry, Maynooth University, Maynooth, Co. Kildare, Ireland
[f] In-Vitro Toxicology Group, Institute of Life Science, Swansea University Medical School, Swansea University, Singleton Park, Swansea, Wales, United Kingdom
[g] Department of Food Biosciences, Teagasc Food Research Centre, Ashtown, Dublin, Ireland
[h] School of Chemical and Biomolecular Engineering, University of Sydney, Australia
[i] The Kathleen Lonsdale Institute of Human Health Research, Maynooth University, Maynooth, Co. Kildare, Ireland

ARTICLE INFO

Article history:
Received 11 May 2021
Received in revised form
28 July 2021
Accepted 29 July 2021
Available online 2 August 2021

Keywords:
Cold atmospheric plasma
Pyrazolopyrimidinone
Pro-drug
ROS
Glioblastoma
Programmable cytotoxicity

ABSTRACT

Pyrazolopyrimidinones are fused nitrogen-containing heterocyclic systems, which act as a core scaffold in many pharmaceutically relevant compounds. Pyrazolopyrimidinones have been demonstrated to be efficient in treating several diseases, including cystic fibrosis, obesity, viral infection and cancer. In this study using glioblastoma U-251MG cell line, we tested the cytotoxic effects of 15 pyrazolopyrimidinones, synthesised via a two-step process, in combination with cold atmospheric plasma (CAP). CAP is an adjustable source of reactive oxygen and nitrogen species as well as other unique chemical and physical effects which has been successfully tested as an innovative cancer therapy in clinical trials. Significantly variable cytotoxicity was observed with IC_{50} values ranging from around 11 μM to negligible toxicity among tested compounds. Interestingly, two pyrazolopyrimidinones were identified that act in a prodrug fashion and display around 5–15 times enhanced reactive-species dependent cytotoxicity when combined with cold atmospheric plasma. Activation was evident for direct CAP treatment on U-251MG cells loaded with the pyrazolopyrimidinone and indirect CAP treatment of the pyrazolopyrimidinone in media before adding to cells. Our results demonstrated the potential of CAP combined with pyrazolopyrimidinones as a programmable cytotoxic therapy and provide screened scaffolds that can be used for further development of pyrazolopyrimidinone prodrug derivatives.

1. Introduction

Despite extensive efforts made in the battle against cancer over the past decades, many challenges remain due to tumour heterogeneity, varied patient characteristics, treatment efficacy, and toxicity considerations. A major limitation in treating advanced carcinoma is delivering sufficient concentrations of a

* Corresponding authors. BioPlasma Research Group, School of Food Science and Environmental Health, Technological University Dublin, Dublin, Ireland.
E-mail addresses: zhonglei.he@tudublin.ie (Z. He), james.curtin@tudublin.ie (J.F. Curtin).

https://doi.org/10.1016/j.ejmech.2021.113736

chemotherapeutic agent to the tumour site without causing undue toxicity elsewhere. For this reason, prodrugs that can be locally activated at the site of the tumour thereby having low toxicity elsewhere are of particular interest.

Reactive oxygen species (ROS), as a natural product generated during normal metabolism pathways, play critical roles in various cellular activities and are considered a carcinogenic factor as high ROS levels are capable of inducing damage and mutation of intercellular DNA and therefore causing malignancy [1]. However, as understanding deepened, ROS was found to be a double-edged sword for cancer cells [2]. Evidence showed that higher ROS levels are generated in cancer cells than healthy cells, which is attributed to the higher metabolic activities and more rapid proliferation of transformed cells [2]. Hence, the cellular antioxidant system works under a more significant load to protect tumour cells from oxidative stress, a common feature in many types of tumours that can be targeted to develop efficient therapies. Attempts have been made to exploit this difference with healthy tissues, and anticancer drugs have been developed that are conditionally activated by high levels of ROS [3]. Cold atmospheric plasma (CAP) can locally induce ROS generation in cells and tissues with a high degree of control of both the amount of ROS generated and the location [4]. CAP treatment has been shown to induce remission of tumour and promote wound healing for head and neck cancer patients in a recent clinical trial [1]. Meanwhile, prodrugs, which only have significant cytotoxicity after being activated by a high ROS level, have fewer side effects and are more specific to cancer cells [5]. Therefore, combining prodrugs with CAP to locally increase tumour ROS and activate cytotoxicity only in tumour tissue may provide a novel promising combination therapy against cancer.

Pyrazolopyrimidinones have been identified with bioactivity for the treatment of cancer [6], infections [7,8], obesity [9,10] and cystic fibrosis [11,12]. It has also been reported that pyrazolopyrimidinones present notable inhibiting effects to the activity or function of several kinases, including the PI3 kinase, glycogen synthase kinase −3 (GSK-3), amongst others. These kinases are involved and can play critical roles in various cellular activities, including cell differentiation, motility, cell growth, proliferation, survival and intracellular trafficking [13–16]. Within this initial structure-activity relationship (SAR) study, 15 pyrazolopyrimidinones have been synthesised and screened for their potential cytotoxic effects combined with CAP treatment, using the glioblastoma U-215MG cell line. Although the IC_{50} value of most cytotoxic candidate, compound **2**, only reached around 11 μM and the majority of them presented moderate, even marginal activity, with or without CAP treatment, two leading prodrug candidates, **9** and **10,** were identified. In combination with low dose CAP treatment, which had negligible toxicity to cancer cells, the cytotoxicity of the leading prodrug candidates **9** and **10** was activated and enhanced by a factor of over 15 fold and 5 fold respectively (IC_{50} against U-251MG cells decreased from around 940 to 62 μM, and 290 to 56 μM, for **9** and **10** respectively). The combination cytotoxicity between **10** and CAP treatment has undergone further investigation, where the ROS generated in culture medium by CAP treatment has been determined to play the primary role in the activation of prodrug **10**. The CAP-induced modification of the compounds are yet explored, but this work provides a potential foundation for further exploration and development of more effective prodrug derivatives based on the screened leading core scaffolds.

2. Materials and methods

2.1. Chemistry general information

All reagents for synthesis were bought commercially and used without further purification. The 3-amino-5-isopropylpyrazole was purchased from Fluorochem and used as received. Reactions were monitored with thin layer chromatography (TLC) on Merck Silica Gel F_{254} plates. NMR spectra were recorded using a Bruker Ascend 500 spectrometer or Bruker 300 Advance spectrometer at 293 K. All chemical shifts were referenced relative to the relevant deuterated solvent residual peaks or TMS. Assignments of the NMR spectra were deduced using ^{1}H NMR and ^{13}C NMR, along with 2D experiments (COSY, HSQC and HMBC). The following abbreviations were used to explain the observed multiplicities; s (singlet), d (doublet), t (triplet), q (quartet), hept (heptet), m (multiplet), bs (broad singlet), pt (pseudo triplet). Flash chromatography was performed with Merck Silica Gel 60. Microwave reactions were carried out using a CEM Discover Microwave Synthesizer with a vertically focused floor mounted infrared temperature sensor, external to the microwave tube. The 10 mL reaction vessels used were supplied from CEM and were made of borosilicate glass. High resolution mass spectrometry (HRMS) was performed on an Agilent-LC 1200 Series coupled to a 6210 or 6530 Agilent Time-Of-Flight (TOF) mass spectrometer equipped with an electrospray source in both positive and negative (ESI+/−) modes. Infrared spectra were obtained as KBr disks in the region 4000–400 cm^{-1} on a PerkinElmer Spectrum 100 FT-IR spectrophotometer. Further experimental details and associated spectra can be found in the Supporting Information.

2.2. Synthesis of pyrazolopyrimidinones

Pyrazolopyrimidinones **1–4, 8, 9, 11, 12** were prepared as described below, NMR spectra can be found in the Supporting Information Figs. S1–S34. Pyrazolopyrimidinones **5–7, 10, 13, 14, 15** were prepared as per the literature procedure reported by Kelada et al. with full experimental details and NMR spectra available in the Supporting Information Fig. S1-S34 [11]. Full experimental details and spectra for the synthesis of the required amino pyrazoles are also found in the Supporting Information.

2.2.1. Synthesis of 2-isopropyl-5-(4-nitrophenyl)pyrazolo[1,5-a] pyrimidin-7(4H)-one (1)

Ethyl 3-(4-nitrophenyl)-3-oxopropanoate (209 mg, 0.88 mmol) was heated at reflux with 3-amino-5-isopropylpyrazole (100 mg, 0.80 mmol) in acetic acid (6 mL) for 6 h. The reaction was cooled to room temperature and the solvent removed under reduced pressure. The residue was dissolved in tetrahydrofuran (THF) (~5 mL) and petroleum ether (40–60 fraction, 5 mL) added. The resulting precipitate was filtered and washed with a minimum of 1:1 mixture of THF: petroleum ether (40–60) to give 2-isopropyl-5-(4-nitrophenyl)pyrazolo [1,5-*a*]pyrimidin-7(4H)-one, 83 mg (58%). ^{1}H NMR: (300 MHz, CD_3OD) δ 8.44 (d, J = 8.6 Hz, 2H), 8.05 (d, J = 8.6 Hz, 2H), 6.19 (s, 1H), 6.16 (s, 1H), 3.12 (m, 1H), 1.37 (s, 3H), 1.35 (s, 3H); ^{13}C NMR: (75 MHz, CD_3OD) δ 164.3, 157.5, 149.5, 148.8, 142.4, 138.7, 128.3, 123.8, 95.0, 86.6, 28.4, 21.4; HRMS: calcd for $C_{15}H_{15}N_4O_3$ m/z: $[M + H]^+$, 299.1139, found: 299.1149 [Diff (ppm) = 3.46].

2.2.2. Synthesis of 5-(3,5-bis(trifluoromethyl)phenyl)-2-butylpyrazolo[1,5-a]pyrimidin-7(4H)-one (2)

Ethyl 3-(3,5-bis(trifluoromethyl)phenyl)-3-oxopropanoate (150 mg, 0.45 mmol) was heated at reflux with 3-butyl-1H-pyrazol-5-amine (63 mg, 0.45 mmol) in acetic acid (2 mL) for 6 h. The reaction was cooled to room temperature and the solvent removed

under reduced pressure. The residue was dissolved in THF (~5 mL) and petroleum ether (40–60 fraction, 5 mL) added. The resulting precipitate was filtered and washed with a minimum of 1:1 mixture of THF: petroleum ether (40–60) to give 5-(3,5-bis(trifluoromethyl)phenyl)-2-butylpyrazolo [1,5-*a*]pyrimidin-7(4H)-one, 43 mg (23%). ^{1}H NMR (300 MHz, CD_3OD) δ 8.44 (s, 2H), 8.24 (s, 1H), 8.32 (s, 1H), 6.22 (s, 1H), 6.18 (s, 1H), 2.78 (t, J = 7.6 Hz, 2H), 1.74 (m, J = 7.6 Hz, 2H), 1.44 (m, J = 7.6 Hz, 2H), 0.98 (t, J = 7.6 Hz, 2H); ^{13}C NMR (75 MHz, CD_3OD) δ 158.7, 157.4, 147.9, 142.4, 135.3, 132.3 (q, J_{CF} = 34.1 Hz), 127.8 (m), 124.3 (m), 123.1 (q, J_{CF} = 272 Hz), 95.1, 88.6, 31.2, 28.0, 22.0, 12.8.

2.2.3. Synthesis of 2-isopropyl-5-(4-methoxyphenyl)pyrazolo[1,5-a]pyrimidin-7(4H)-one (3)

A microwave tube was charged with ethyl 4-methoxybenzoyl acetate (0.17 mL, 0.9 mmol), 3-amino-5-isopropylpyrazole (110 mg, 0.9 mmol), and methanol (2 mL) and subjected to microwave irradiation (100 W, 120 °C) for 1 h. At this point, three drops of acetic acid were added, and the reaction mixture subjected to microwave irradiation (100 W, 120 °C) for a further 2 h. The resultant precipitate was removed by filtration and washed with a minimum amount of cold methanol, giving 42 mg of 2-isopropyl-5-(4-methoxyphenyl)pyrazolo [1,5-*a*]pyrimidin-7(4H)-one. The filtrate was evaporated to dryness and the resulting residue recrystallised from methanol to give a further 85 mg of 2-isopropyl-5-(4-methoxyphenyl)pyrazolo [1,5-*a*]pyrimidin-7(4H)-one. The combined yield was 127 mg (50%). ^{1}H NMR: (300 MHz, DMSO-d_6) δ 12.21 (s, 1H, NH), 7.79 (d, J = 8.9 Hz, 2H), 7.13 (d, J = 8.9 Hz, 2H), 6.03 (s, 1H), 5.95 (s, 1H), 3.85 (s, 3H), 3.01 (m, 1H), 1.28 (s, 3H), 1.26 (s, 3H); ^{13}C NMR: (75 MHz, DMSO-d_6) δ 161.8, 161.4, 156.3, 142.1, 128.7, 114.4, 92.5, 86.4, 55.5, 27.9, 22.3; HRMS: calcd for $C_{16}H_{18}N_3O$ m/z: $[M + H]^+$, 284.1394, found: 284.1388 [Diff (ppm) = 2.05].

2.2.4. Synthesis of 5-(3,5-bis(trifluoromethyl)phenyl)-2-isopropylpyrazolo[1,5-a]pyrimidin-7(4H)-one (4)

A microwave tube was charged with 3-isopropyl-1H-pyrazol-5-amine (113 mg, 0.9 mmol), ethyl 3-(3,5-bis(trifluoromethyl) phenyl)-3-oxopropanoate (295 mg, 0.9 mmol), acetic acid (28.6 μL, 0.5 mmol), MeOH (1 mL), and subjected to MW irradiation (100 W, 150 °C) for 2 h. The resulting mixture was concentrated in vacuo and purified by trituration with cold ethyl acetate to give 5-(3,5-bis(trifluoromethyl)phenyl)-2-isopropylpyrazolo [1,5-*a*]pyrimidin-7(4H)-one, 140 mg (40%). ^{1}H NMR (500 MHz, DMSO-d_6) δ 12.65 (bs, 1H), 8.51 (s, 2H), 8.32 (s, 1H), 6.30 (s, 1H), 6.10 (s, 1H), 3.05–2.95 (m, J = 13.5, 6.7 Hz, 1H), 1.25 (d, J = 6.8 Hz, 6H); ^{13}C NMR (126 MHz, DMSO-d_6) δ 162.4, 156.1, 146.3, 142.1, 135.0, 131.1 (q, J_{CF} = 33.3 Hz), 128.5, 124.4, 123.2 (q, J_{CF} = 273.4 Hz), 95.5, 86.9, 28.0, 22.3; Rf 0.5 (1:9 v/v MeOH:EtOAc); HRMS: calcd for $C_{17}H_{14}F_6N_3O$ m/z, [M + H]+, 390.1036, found: 390.1051, [Diff (ppm) = 2.79]; IR (KBr): 3423 (*N*–H), 2972 (*C*–H), 1670 (C=O), 1617 (C=C), 1577 (*N*–H), 1481 (C=C), 1279 (*C*–F), 1139 (*C*–N) cm^{-1}.

2.2.5. Synthesis of 2-isopropyl-6-methyl-5-phenylpyrazolo[1,5-a]pyrimidin-7(4H)-one (8)

Ethyl 2-methyl-3-oxo-3-phenylpropanoate (125 mg, 0.61 mmol) was heated at reflux with 3-amino-5-isosubstitutedpyrazole (69 mg, 0.55 mmol) in acetic acid (2 mL) for 15 h. The reaction was allowed to cool to room temperature and the solvent removed under reduced pressure. The residue was triturated with ethyl acetate to yield a solid. The solid was isolated by filtration, washed with ethyl acetate, and dried in a drying pistol to give 2-isopropyl-6-methyl-5-phenylpyrazolo [1,5-*a*]pyrimidin-7(4H)-one, 54 mg (37%). ^{1}H NMR (500 MHz, MeOD) δ 7.70–7.45 (m, 5H), 5.98 (s, 1H), 3.08 (hept, J = 7.0 Hz, 1H), 2.00 (s, 3H), 1.32 (d, J = 7.0 Hz, 6H). ^{13}C NMR (126 MHz, MeOD) δ 164.0, 163.9, 158.7, 148.0, 141.6, 141.5, 133.8, 129.8, 128.5, 128.4, 101.7, 101.7, 84.7, 28.4, 28.4, 21.6, 10.7; HRMS: calcd for $C_{16}H_{18}N_3O$ m/z, [M + H]+, 268.1444, found: 268.1452, [Diff (ppm) = 2.95].

2.2.6. Synthesis of 2,5-di-tert-butylpyrazolo[1,5-a]pyrimidin-7(4H)-one (9)

The amino pyrazole 5-amino-3-(*tert*-butyl)-1H-pyrazole (100 mg, 0.71 mmol) was dissolved in acetic acid (10 mL), and ethyl 4,4-dimethyl-3-oxopentanoate (116 μL, 0.65 mmol) added. The reaction mixture was heated at reflux overnight. After cooling to rt, the acetic acid was removed under reduced pressure and trituration with ethyl acetate (5 mL) gave 2,5-di-*tert*-butylpyrazolo [1,5-*a*] pyrimidin-7(4H)-one, 42 mg (23 %). ^{1}H NMR: (300 MHz, CD_3OD) δ 6.08 (s, 1H, H5), 5.74 (s, 1H, H2), 1.38 (s, 18H, $(CH_3)_3 \times 2$); ^{13}C NMR: (125 MHz, CD_3OD) δ 166.7, 161.6, 158.5, 142.2, 91.3, 85.4, 34.9, 32.4, 29.2, 27.6; R_f: 0.6 (1:9 v/v, MeOH:DCM); HRMS: calcd for $C_{14}H_{22}N_3O$ m/z, $[M + H]^+$, 248.1757, found: 248.1768, [Diff (ppm) = 4.45]; IR (KBr): 3090 (*N*–H), 2965 (*C*–H), 1670 (C=O), 1614 (C=C), 1570 (*N*–H), 1481 (C=C), 1240 (*C*–N) cm^{-1}.

2.2.7. Synthesis of 5-(3,5-dimethylphenyl)-2-methylpyrazolo[1,5-a]pyrimidin-7(4H)-one (11)

Ethyl 3-(3,5-dimethylphenyl)-3-oxopropanoate (0.56 mL, 3.0 mmol) was added to a solution of 3-amino-5-methylpyrazole (132 mg, 1.0 mmol) dissolved in acetic acid (5 mL) and heated at reflux for 21 h. Volatiles were removed under reduced pressure. The product was purified by column chromatography (100% DCM) to give 5-(3,5-dimethylphenyl)-2-methylpyrazolo [1,5-*a*]pyrimidin-7(4H)-one, 204 mg, (59 %). ^{1}H NMR: (500 MHz, CD_3OD) δ 7.42 (s, 2H), 7.26 (s, 1H), 6.13 (s, 1H), 6.05 (s, 1H), 2.53–2.34 (m, 9H); ^{13}C NMR: (126 MHz, CD_3OD) δ 138.9, 132.3, 124.5, 19.9; HRMS: calcd for $C_{13}H_{16}N_3O$ m/z, [M + H]+, 254.1293' found: 253.1207, [Diff (ppm) = 3.3]; Rf: 0.11 (100 % DCM); IR (KBr): 3251 (*N*–H), 2917 (*C*–H), 1665 (C=O), 1618 (*N*–H), 1597 (Ar *C*–C) cm^{-1}.

2.2.8. Synthesis of 5-(3,5-dimethylphenyl)-2-isopropylpyrazolo[1,5-a]pyrimidin-7(4H)-one (12)

Ethyl 3-(3,5-dimethylphenyl)-3-oxopropanoate (28 mL, 1.4 mmol) was added to a solution of 3-isopropyl-1*H*-pyrazol-5-amine (176 mg, 1.4 mmol) dissolved in acetic acid (5 mL) and refluxed for 5.5 h. Volatiles were removed under reduced pressure. The product was purified by trituration using ethyl acetate (10 mL) and give 5-(3,5-dimethylphenyl)-2-isopropylpyrazolo [1,5-*a*]pyrimidin-7(4H)-one, 165.4 mg (42 %). ^{1}H NMR: (500 MHz, $CDCl_3$) δ 9.51 (bs, 1H), 7.25 (s, 2H), 7.13 (s, 1H), 6.00 (m, 2H), 3.10 (septet, 1H), 2.34 (s, 6H), 1.28 (d, J = 7.0 Hz, 6H); ^{13}C NMR: (126 MHz, $CDCl_3$) δ 157.8, 141.6, 139.1, 132.8, 132.7, 124.5, 94.6, 86.7, 28.6, 22.5, 21.3; HRMS: calcd for $C_{17}H_{20}N_3O$ m/z: $[M + H]^+$, 281.1528, found: 281.1528 [Diff (ppm) = 0.06]; IR (KBr): 3199 (*N*–H), 3081 (*C*–H), 1651 (C=O), 1595 (*N*–H), 1291 (Ar *C*–N) cm^{-1}.

2.3. Cell culture

U-251 MG (formerly known as U373MG) (ECACC 09063001), human brain glioblastoma cancer cells (Obtained from Dr Michael Carty, Trinity College Dublin) and HEK293, human embryonic kidney cells (Obtained from Dr Darren Fayne, Trinity College Dublin) were cultured in DMEM-high glucose medium (Merck, D6429) supplemented with 10 % FBS and maintained in a 37 °C incubator within a humidified 5 % (v/v) CO_2 atmosphere. For prodrug treatment, DMEM-high glucose medium without pyruvate (Merck, D5796) was used to make up culture medium to avoid the antioxidant effects of pyruvate [17].

2.4. H_2DCFDA assay

H_2DCFDA was used to detect ROS induced by CAP treatment. U-251 MG cells were seeded into 35 × 10 mm tissue culture dishes (Sarstedt) at a density of 2×10^5 cells/ml, or 35 mm glass-bottom dishes (Greiner Bio-One) at a density of 1×10^5 cells/ml and incubated overnight as above to allow adherence. Prior to treatment with CAP at 75 kV for 30 s, cells were first incubated with 25 μM H_2DCFDA (Thermo Fisher Scientific) in serum-free medium for 30 min at 37 °C, then washed with phosphate buffered saline (PBS) twice, culture medium once. Afterwards, cells were observed under a Zeiss LSM 510 confocal laser scanning microscope (excitation 488 nm, emission 505–530 nm), or were collected for measurement with flow cytometry.

2.5. CAP configuration and prodrug treatment

An experimental atmospheric dielectric barrier discharge (DBD) plasma reactor, DIT-120, was used which has been described and characterised in detail elsewhere [18,19]. Unless otherwise stated, all U-251 MG cells were treated within 96-well plates. During CAP treatment, containers were placed in between two electrodes, at a voltage level of 75 kV for 10–40 s. The culture medium was removed before CAP treatment then replaced with fresh culture medium immediately afterwards.

An optimised prodrug treatment protocol was developed and applied, as described below. U-251 MG cells were plated into 96-well plates (Sarstedt) at a density of 1×10^4 cells/well (100 μl standard culture medium per well) and were incubated overnight for proper adherence. Unless otherwise stated, the plating map was 6 × 10 wells, for ten different concentrations, negative and positive control groups (5 replicates for each group). All prodrugs were dissolved and prepared in 100 % DMSO for the stock solution, which was then serially diluted in culture medium to different concentrations as indicated. 10 μl of prodrug non-pyruvate culture medium solution was then added to each well after removing the previous medium, and the remainder was added into empty wells in the plate. The plate then was treated with CAP at 75 kV for 10–40 s as indicated. 90 μl of CAP-treated prodrug culture medium solution was then added to corresponding wells with cells to final volume 100 μl immediately after CAP treatment. Cell viability assays were then carried out following incubation for the indicated time. Temozolomide (TMZ) (Merck) was dissolved in DMSO as stock (50 mM) and then subsequently diluted in culture medium to concentrations as indicated. U-251 MG cells were plated into 96-well plates at a density of 2×10^3 cells/well and were incubated overnight to ensure proper adherence. The combination treatment of TMZ and 30 s CAP was performed with the same method as above. Meanwhile, the TMZ stock was first treated with CAP for 15 min then diluted in culture medium to indicated concentrations and incubated with untreated cells, for six days, as indicated.

Indirect CAP treatment was used to investigate the effects of CAP on pro-drugs alone to determine the mechanism of combination cytotoxicity to U-251 MG cells. Pro-drugs were treated with CAP at 75 kV for 10 s to 10 min in DMSO stock solution or culture medium solution as indicated. The CAP-treated prodrug solution was then added to U-251 MG cells in 96-well plates to incubate with U-251 MG cells. For CAP-activated medium, the culture medium was treated with CAP at 75 kV for 30 s in 96-well plate and incubated overnight at 4 °C to remove short-lived reactive species. The prodrug stock solution was then serially diluted in the overnight storage CAP-activated medium and incubated with U-251 MG cells. For CAP-activated cells, the U-251 MG cells overlaid with 10 μl culture medium were treated with CAP for 30 s in 96-well plates, while remainder of culture medium was added into empty wells in the plate. Then the CAP-treated culture medium was added to each well to 100 μl. Those CAP-activated cells were then incubated in the CAP-activated medium for 0–5 h as indicated. Following incubation, the medium was replaced with fresh medium containing corresponding concentrations of prodrugs. ROS generator, 2,2′-azobis (2-amidinopropane) dihydrochloride (AAPH, purchased from Merck), was dissolved in water to 0.5 M as stock solution and kept at −20 °C till use. The AAPH stock solution was diluted in pyruvate-free culture medium to desired concentrations then incubated with HEK293 or U-251MG cells combined with prodrugs for indicated hours before Alamar Blue assays.

2.6. Cytotoxicity and inhibitor assays

Cell viability was analysed using the Alamar blue assay (Thermo Fisher Scientific). 48 h after CAP treatment, the cells were rinsed once with PBS, incubated for 3 h at 37 °C with a 10 % Alamar blue/90 % culture medium solution. The fluorescence was then measured (excitation, 530 nm; emission, 595 nm) by a Victor 3 V 1420 microplate reader (PerkinElmer). 4 M *N*-Acetyl Cysteine (NAC) stock solution was prepared in water. 4 M NAC solution was then diluted in culture medium to a final concentration of 4 mM before the addition of prodrugs and CAP treatment. The CAP treated culture medium containing prodrugs and 4 mM NAC was then added into 96-well plates to incubate with U-251 MG cells.

2.7. Live/dead staining

U-251MG cells were seeded in 96-well plate at a density of 1×10^4 cells/well and allow overnight for adherent, as described above. Cells were then treated with 2000, 290 and 0.3 μM of **10** respectively in culture medium without pyruvate for 48 h. The live/dead staining was performed with LIVE/DEAD™ Viability/Cytotoxicity Kit, for mammalian cells (ThermoFisher). In brief, after 48-h incubation with compounds, the previous medium was removed and a staining PBS solution containing 2 μM of Calcein-AM and 4 μM of ethidium homodimer-1 (EthD-1) was added and incubated at room temperate for 30 min, prior to fluorescent imaging (excitation/emission: Calcein-AM 494/517 nm; EthD-1528/617 nm).

2.8. Statistical analysis

Triplicate independent tests were carried out for each data point unless indicated otherwise. Error bars of all figures are presented using the standard error of the mean (S.E.M). Prism 7 (GraphPad Software, San Diego, CA, USA) was used to carry out curve fitting and statistical analysis. The isobologram was carried out using CompuSyn software (ComboSyn, Inc., Paramus, NJ, USA, www.combosyn.com) [20]. Two-tailed P values were used where alpha = 0.05. The significance between data points was verified using one-way ANOVA and two-way ANOVA with Tukey's multiple comparison post-test, as indicated in figures (*P < 0.05, **P < 0.01, ***P < 0.001, ****p < 0.0001).

3. Results

3.1. ROS generation by low dose CAP treatment

CAP has been well known for inducing the generation of ROS [19,21,22]. In addition to flow cytometry, we have used a confocal microscope and ROS indicator H_2DCFDA to demonstrate the ROS generated by 30 s of CAP treatment (Fig. 1A and B). 30 s of CAP treatment is a small dose presenting relatively low cytotoxicity to U-251 MG cell lines, with only a decrease of around 20 % in cell viability as previously described [19,21]. As seen in Fig. 1C, 0-40 s of

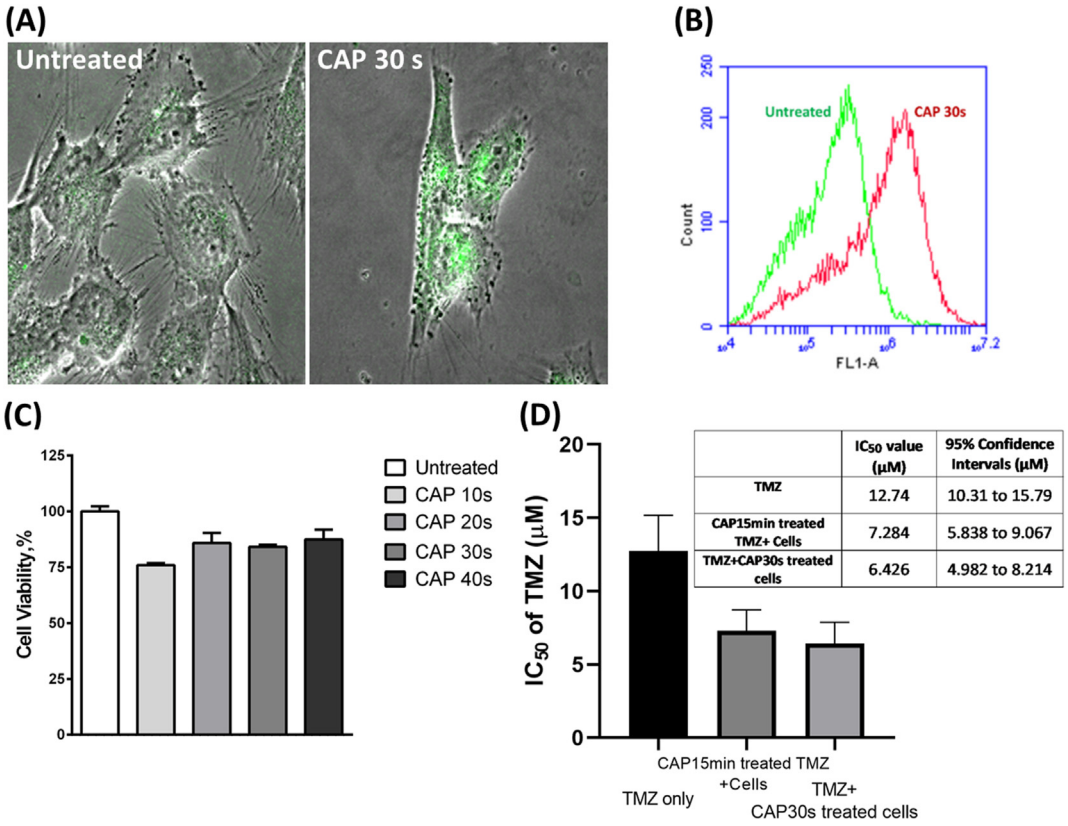

	IC_{50} value (μM)	95% Confidence Intervals (μM)
TMZ	12.74	10.31 to 15.79
CAP15min treated TMZ+ Cells	7.284	5.838 to 9.067
TMZ+CAP30s treated cells	6.426	4.982 to 8.214

Fig. 1. Treatment of U-251 MG cells with reactive species-generating CAP treatment alone or in combination with TMZ. (**A**) Fluorescence levels of oxidised H_2DCFDA in untreated and 30s CAP treated cells were observed via confocal microscope. (**B**) Fluorescence level of intracellular oxidised H_2DCFDA was measured in U-251 MG cells via Flow cytometry, left curve (green, untreated cells), right curve (red, 30 s CAP treated cells). (**C**) U-251 MG cells were treated with CAP for 10–40 s at 75 kV alone and then incubated for 48 h before cell viability was assessed. (**D**) CAP untreated or CAP 30s treated U-251 MG cells were incubated with a serial dilution of TMZ only or 15min CAP treated TMZ stock solution for 6 days, Cell viability assays were then carried out, and IC_{50} values were calculated using GraphPad Prism.

CAP treatment decreased around 10–20 % of cell viability when U-251 cells were treated and incubated in the culture medium without pyruvate. TMZ, the standard chemotherapy for glioblastoma, has been tested in combination with 30 s and 15 min of CAP treatment on cells or TMZ stock solution separately. CAP has previously been demonstrated to restore drug sensitivity in cisplatin-resistant ovarian cancer cells [23], paclitaxel-resistant breast cancer cells [24], tamoxifen-resistant breast cancer cells [25], and temozolomide-resistant malignant glioma cells [26]. As seen in Fig. 1D, there is a marginal decrease of IC_{50} values of TMZ when U-251 MG cells were treated with both TMZ and 30s of CAP treatment, which is in agreement with previously published studies demonstrating that CAP possesses an ability to restore the sensitivity of U-251 MG cells to TMZ [19,26]. We also found that 15 min of CAP treatment on TMZ stock solution did not induce a significant degradation of TMZ cytotoxicity. Instead, we observed a similar marginal decrease in IC_{50} values (Fig. 1D and Supporting Information Fig. S35).

On the other hand, some pyrazolopyrimidines were found to be involved in cellular ROS generation. (4-Amino-6-hydroxypyrazolo-3,4-*d*-pyrimidine) was found to inhibit xanthine oxidase and decrease the enzymatic formation of uric acid and ROS [27]. Another pyrazolopyrimidine was demonstrated to generate ROS in NCI–H460 (non-small-cell lung cancer) cells, leading to a loss in mitochondrial membrane potential and apoptosis of the cancer cells [28]. Therefore, in this initial SAR study, 15 pyrazolopyrimidinones were selected to study their cytotoxicity against U-251 MG cells, and more specifically the possible prodrug activation effects with ROS generating CAP treatment.

3.2. Screening of pyrimidone bicycle family compounds

As described in the Methods section and Supporting Information 15 pyrazolopyrimidinone compounds were synthesised in a two-step process, via an aminopyrazole intermediate, from the corresponding keto nitrile and keto ester (Fig. 5). The cytotoxicity of the compounds was evaluated in combination with small doses of CAP treatment in order to identify possible candidates that are activated by CAP (via restoring cellular sensitivity or a ROS-dependent prodrug effect). As seen in Fig. 2, most pyrazolopyrimidinones had no activated cytotoxicity when the compounds, together with cells in media, were directly treated by CAP for 30 s in media. The dose-response curves of CAP-treated groups presented high comparability and similar trends with untreated groups, as 30 s of CAP treatment presents negligible or low cytotoxicity when applied alone. On the other hand, two compounds from the pyrazolopyrimidinone family, **9** and **10**, presented significant activated cytotoxicity in combination with 30 s of direct CAP treatment (Fig. 2). The CAP treatment induced a pronounced descent of dose-response curves with increasing compound concentration. As seen in Table 1, CAP treatment induced significant decreases of IC_{50} values of **9** (from 940.6 μM to 62.41 μM) and **10** (from 292.8 μM to 56.79 μM) while presenting low cytotoxicity by themselves. Therefore, among all 15 candidates, **9** and **10** were determined as

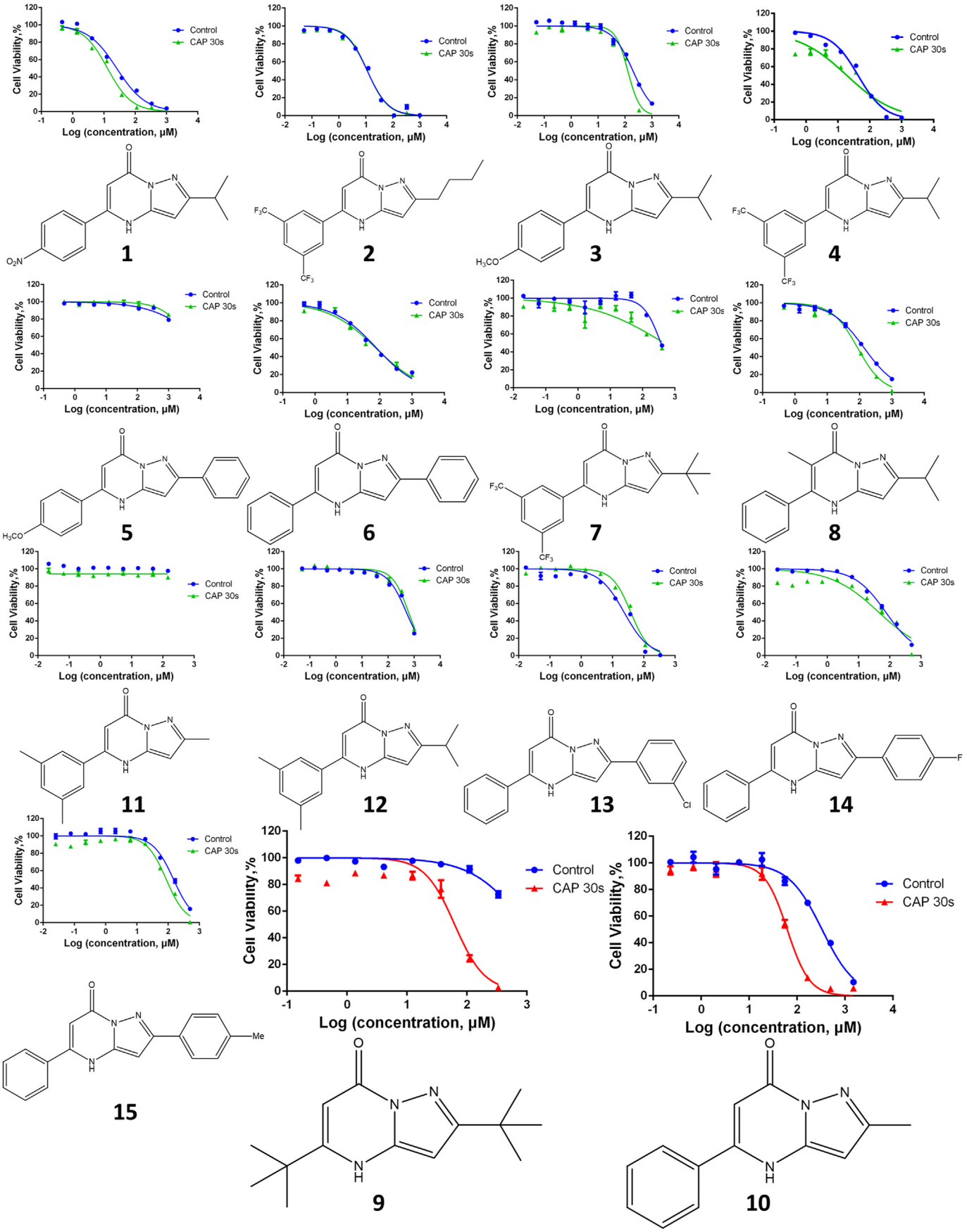
Cell Viability,%
Log (concentration, μM)
Control
CAP 30s
1
2
3
4
5
6
7
8
11
12
13
14
15
9
10

the leading candidates with potential as CAP-activated drugs.

One can notice that the 95 % confidence intervals for of compounds 5 (both groups) and 9 (control groups) were large. This is due to that the cell viability of upper end of the dose ranges was still lower than 50 %, demonstrating their limited activity against glioblastoma cell lines. Thus, the IC_{50} value was calculated via non-linear regression using GraphPad Prism, which gave large 95 % confidence intervals in this case. The dose ranges were limited by the solubility of compounds in DMSO, as well as the limited dilution of DMSO stock in culture media.

3.3. Plasma activated media enhances cytotoxicity of leading prodrug candidate

We selected **10** to investigate further the prodrug activated cytotoxic effects combined with CAP treatment. Live/dead staining was performed to further determine the status of cells in addition to Alamar Blue assay. After incubation with 0.3, 290 and 2000 μM of **10** for 48 h, around 100 %, 50 % and 10 % cell viability was determined by Alamar Blue assay. As seen in Fig. 3, a significant decrease of living cells stained with green (Calcein-AM) and a moderate increase of dead cells stained with red (ethidium homodimer-1, EthD-1) was observed from 100 % to 10 % groups. Also, distinct morphological changes was demonstrated in 10 % cell viability group. Thus, **10** may decrease the cell viability via cytotoxicity along with inhibition of proliferation, in which the cell death pathways are awaiting further exploration. In addition, the cytotoxicity of **10** against HEK293 cells was tested compared to U-251MG cells, and a slightly higher cytotoxic effect in HEK293 cells (IC_{50},123.3 μM, 95 % confidence intervals, 111.5—136.5 μM) was observed (Supporting Information Fig. S36).

On the other hand, the prodrug activation mechanism was investigated. **10** was first dissolved in 100 % DMSO to 200 mM and then treated with 30 s and 10 min of CAP. Afterwards, CAP-treatment **10** DMSO solution was diluted in the culture medium to incubate with cells. As seen from Fig. 4A and Table 2, no significant increase in cytotoxicity was observed whether the **10** DMSO solution was treated with CAP or not. ROS generation is absent in 100 % DMSO solvent, whereas the generation of reactive species relies on the presence of reactants in treated liquid [29], and DMSO may function as a scavenger of OH radicals [30]. Therefore, we hypothesised that ROS generation might be essential for the activation of compound **10**.

10 was then diluted in culture medium first and treated with CAP in 10 s increments from 0 s to 40 s. The CAP-treated **10** culture medium solution was subsequently incubated with U-251 MG cells for 48 h before the Alamar Blue assay. As seen in Figs. 1C and 4B and Table 3, CAP 10—40 s treated **10** culture medium solution induced a pronounced decrease of cell viability with concentrations higher than 10 μM compared to cells treated with media not exposed to CAP. CAP treatment of media alone had low cytotoxicity (~20 % decrease in cell viability, Fig. 1C). Meanwhile, NAC was applied as an antioxidant to investigate the mechanism further. The 4 M NAC solution was diluted in the culture medium to 4 mM before adding **10** and 40 s CAP treatment. As seen in Fig. 4B and Table 3, the NAC and CAP treated group presented much higher cell viability and a higher IC_{50} value than the CAP treated groups, which demonstrated that ROS generated in culture media by CAP treatment played an essential role in activating the effect of **10** against U-251MG cells. Using CompuSyn software, the normalised isobologram was analysed, and the combination index (CI) values have been calculated to evaluate the combination treatment. The CI values of **10** were 0.31099 with 10 s, 0.33520 with 20 s, 0.47561 with 30 s, and 0.57796 with 40 s of CAP treatment, which were all less than 1.00 and confirmed the significant prodrug activation effect (Fig. 4C). **11**, which is structurally similar to compound **10**, two *meta* methyl substituents added to the pheny ring, was also tested for comparison. Interestingly, as seen in Supporting Information Fig. S37a**, 11** showed no enhanced cytotoxicity when treated in culture medium with CAP for 10—40 s, which suggests an important role for the phenyl ring of the pyrazolopyrimidinone.

Our results demonstrate that **10** was activated by reactive species generated during CAP treatment, therefore presenting significant activated cytotoxicity to U-251 MG cells when combined with CAP treatment. Furthermore, overnight storage CAP-activated medium and CAP-activated cells have been used to study the dose-response of U-251 MG cells to **10**. When cells were treated with overnight storage CAP-activated medium and prodrug, no activation was observed (Supporting Information Fig. S37b). Meanwhile, when the U-251 MG cells were incubated for 0 h—5 h after CAP treatment, then incubated with fresh medium containing prodrug, there was no significant activation of the prodrug observed, either (Supporting Information Fig. S37c). In addition, a ROS generator, AAPH, was used to test its potential activation effect towards **10.** AAPH is a stable compound that constantly generates peroxyl radicals (ROO•) at 37 °C in aqueous solution for several hours and is considered to induce reliable oxidative stress model [31,32]**.** Interestingly, in U-251MG and HEK293 cell lines, the addition of 3 mM AAPH in pyruvate free culture medium, which only decrease 20 % cell viability alone, significantly decreased cell viability to 50 % combined with low concentrations of **10.** However**,** the cytotoxicity of **10** was not enhanced when the concentration is above 200 μM (Supporting Information Figs. S36a, b, e). When the prodrug **10** was co-incubated with 0.5 mM of AAPH, no enhanced cytotoxicity was observed in both cell lines (Supporting Information Figs. S36c and d).

4. Discussion and conclusions

Despite improvements in precision surgery, targeted and focused chemotherapy and radiotherapy, emerging immunotherapy, and quick and accurate diagnosis of tumours, cancer mortality remains a significant global health burden, accounting for almost 10 million deaths in 2018, or 1 in 6 of all mortalities [33]. Current primary treatments still present several side effects when applied alone with high doses, including poor patient experience, secondary malignancy and a variety of long-term sequelae [2,34—36]. In this case, combination therapy has been considered a promising approach to target tumours while generating fewer side effects.

With the altered metabolism and rapid proliferation, the high ROS level in cancer cells is considered a promising target for developing specific therapies [37]. The chemotherapy agents related to ROS can be divided into ROS-trigger drugs and ROS-activated drugs. ROS-trigger drugs can further increase the ROS level in cancer cells beyond their tolerable allowance to trigger cell death, such as fenretinide [38], nitric oxide-donating aspirin [39], imexone [40] and motexafin gadolinium [41]. On the other hand, ROS-activated drugs, also termed prodrugs, can be activated and become cytotoxic by the relative high ROS level in cancer cells,

Fig. 2. Dose response curves of Pyrazolopyrimidinones. The stock solution of pyrazolopyrimidinones 1—15 were prepared in 100 % DMSO, which was then serially diluted in culture medium without pyruvate to different concentrations as indicated. U-251 MG cells were treated with 1—15 in combination with 30 s of CAP treatment as indicated in the Methods section. Cell viability assays were then carried out following incubation with 1—15 culture medium solution for 48 h.

Table 1
IC_{50} values and 95 % confidence intervals of pyrazolopyrimidinones alone or in combination with 30 s of CAP treatment against U-251 MG cells.

	Control			CAP 30 s		
Compound number	IC_{50} (μM)	Hillslopes	95 % Confidence Intervals (μM)	IC_{50} (μM)	Hillslopes	95 % Confidence Intervals (μM)
1	25.51	−0.9429	22.84 to 28.50	12.92	−1.125	11.53 to 14.48
2	11.32	−1.121	10.09 to 12.70	11.4	−1.159	10.34 to 12.57
3	197	−1.149	174.3 to 222.7	126.8	−1.918	113.0 to 142.4
4	42.9	−1.043	37.75 to 48.74	19.04	−0.5718	13.75 to 26.38
5	13,372	−0.5624	5733 to 31,190	5670	−1.007	1831 to 17,555
6	77.68	−0.6622	66.55 to 90.67	73.62	−0.5991	60.59 to 89.44
7	366.8	−1.649	306.1 to 439.5	462.1	−0.3780	197.3 to 1082
8	137.2	−0.8449	120.2 to 156.6	86.27	−1.100	76.20 to 97.68
9	940.6	−0.9807	564.2 to 1568	62.41	−1.741	49.58 to 78.56
10	292.8	−1.344	252.2 to 340.0	56.79	−2.198	50.93 to 63.33
11	Not converged			Not converged		
12	502.2	−1.201	452.4 to 557.4	608.6	−1.432	561.0 to 660.2
13	23.34	−1.101	19.82 to 27.49	38.23	−1.475	34.96 to 41.80
14	74.59	−0.8717	67.68 to 82.20	44.42	−0.5734	31.39 to 62.85
15	148.1	−1.340	131.7 to 166.6	86.7	−1.406	75.02 to 100.2

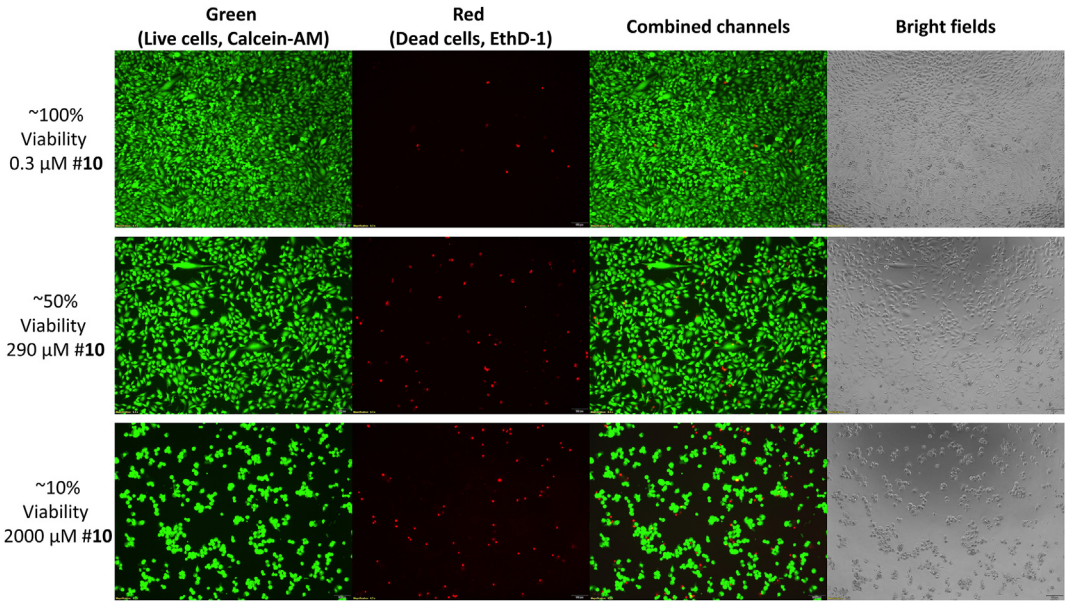

Fig. 3. Live/dead staining of U-251MG cells. ~100 %, 50 % and 10 % cell viabilities were achieved by inucabating cells with 0.3, 290 and 2000 μM of compound 10 for 48 h.

leading to specific cancer cell killing effects. Meanwhile, CAP, a novel technology allows a localised generation of ROS at a tumour site, has been demonstrated to have significant therapeutic potential in cancer treatment [1,42–44]. In this case, CAP provides the ideal mechanism to augment or activate ROS-sensitive pro-drugs in targeted areas.

Modifying bioactive scaffold cores with functional groups or linkers that can be specifically activated and altered is a common strategy to develop prodrugs. A novel imidazopyridazine, with a sulfoxide/sulfone prodrug-like strategy, was found to cure mice infected with *P. berghei* parasites at 4 × 50 mg/kg, when the methylsulfoxide derivative rapidly generated the methylsulfone derivative in vivo, leading to higher plasma exposure compared to direct use of the methylsulfone derivative [45]. Hybrids of two active compounds via a prodrug linker has also been exploited as combination treatments. Rapamycin derivatives have been conjugated with hydroxywortmannin via linkers like diester bond for potential synergistic efficacy of concomitant inhibition of PI3K and mTOR for cancer treatment [46].

On the other hand, many pyrazolopyrimidines have found use in drug development and have potential in antiviral, antimicrobial, anticoccidials, antitumour and anti-inflammatory activities [47]. Pyrazolopyrimidine derivatives have been found to inhibit many protein kinases, such as Src kinase [48], cyclin-dependent kinases [49,50], Chk1 Checkpoint kinase [51], B-Raf protein kinase [52] and Aurora-A kinase [53], which are considered significant targets for anticancer drug development, as the alterations in many kinase activities are involved in cancerous mutations [54]. The potential interactions between this diversified family and ROS have also been noted [27,28].

Therefore, 15 pyrazolopyrimidinones, a class of pyrazolopyrimidine derivatives, were selected to study their possible prodrug activation effects combined with ROS-generating CAP treatment. The pyrazolopyrimidinones were synthesised using a two-step process (Fig. 5), which involved generating an isolatable amino pyrazole intermediate (step one) and its subsequent reaction with the corresponding β-ketoester to give the desired pyrazolopyrimidinone (step two) [11]. A family of pyrazolopyrimidinones was generated, which incorporated structural variation at R1 (R1 = phenyl, substituted aryl, or alkyl groups) and R^2 (R^2 = phenyl, substituted aryl, or alkyl groups). The pyrazolopyrimidinones were generated in 16–67 % yields and underwent structural

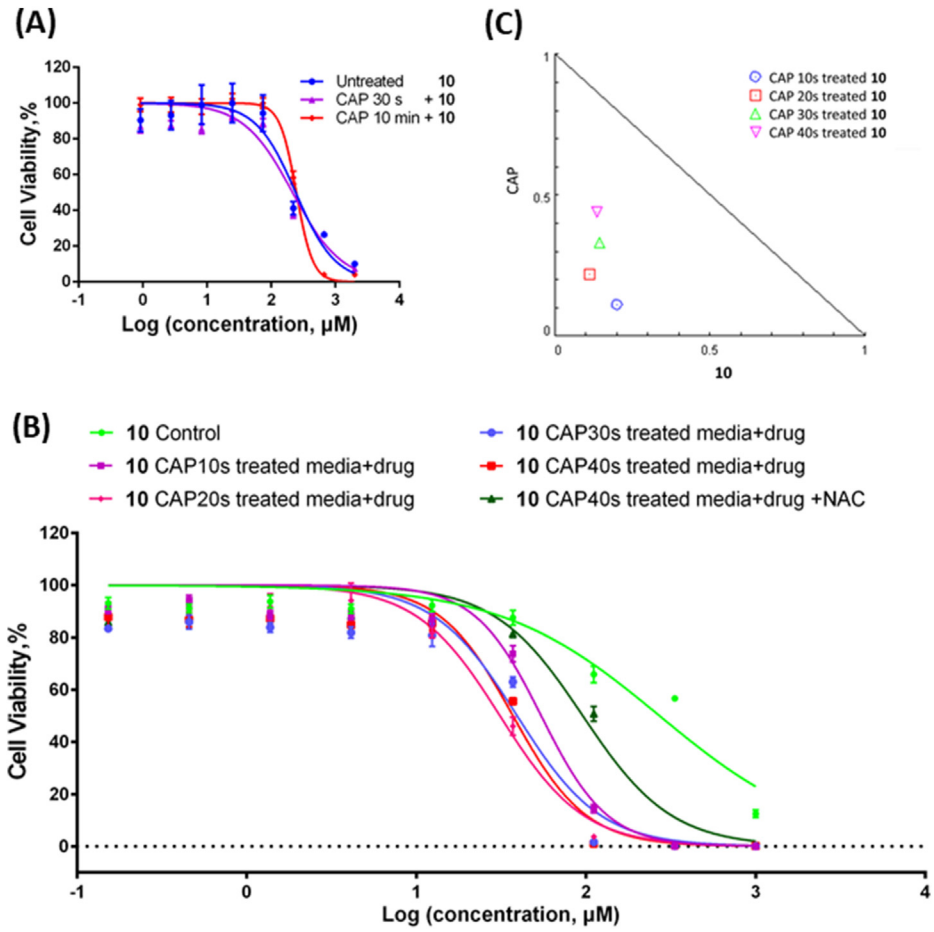

Fig. 4. Dose responses of U-251 MG cells to 10 treated by CAP in culture medium solution or DMSO stock solution. (**A**) **10** was prepared in DMSO stock solution and treated with CAP for 30 s and 10 min, serially diluted into fresh culture medium and incubated with U-251 MG cells for 48 h and compared with control groups. (**B**) **10** was prepared in the culture medium, treated with CAP for 0–40 s with or without NAC and then incubated with U-251 MG cells in 96-well plates for 48 h before cell viability was assessed. (**C**) Isobologram analysis of the combinational effect of **10** and CAP. The single doses CAP on the y-axis and **10** on the x-axis were used to draw the additivity line. Four combination points were indicated in the isobologram (CAP 10–40s and corresponding IC_{50} values of CAP-treated **10**). The localisation of combined **10** and CAP at different time exposures can be translated to synergism CI < 1, additivity CI = 1 or antagonism CI > 1.

Table 2
IC_{50} values of 10 treated by CAP in DMSO solution.

	IC_{50} (μM)	95 % Confidence Intervals (μM)	Hill Slopes
10 **Control (2**nd **repeat)**	240.5	170.8 to 338.8	−1.408
CAP 30 s treated 10 **(In DMSO)**	215.3	169.4 to 273.5	−1.139
CAP 10 min treated 10 (In DMSO)	246.0	235.4 to 257.1	−3.385

Table 3
IC_{50} values of 10 treated by CAP 0–40s in culture medium solution.

	IC_{50} (μM)	95 % Confidence Intervals (μM)	HillSlopes
10 **Control (3**rd **repeat)**	270.9	218.6 to 335.6	−0.9283
10 **CAP10s**	54.37	47.56 to 62.15	−2.228
10 **CAP20s**	31.05	26.71 to 36.10	−1.764
10 **CAP30s**	39.21	31.27 to 49.16	−1.765
10 **CAP40s**	37.06	31.18 to 44.04	−2.012
10 **CAP40s + NAC**	95.65	79.08 to 115.7	−1.667

characterised using NMR spectroscopy, IR spectroscopy, and mass spectrometry (see Method section and Supporting Information). The majority of candidates showed moderate to marginal cytotoxic effect towards tumour cells when applied alone or in combination with 30 s of CAP treatment. Although the IC_{50} values presented no significant cytotoxicity alone or promising specific tumour cell-killing efficacy (Table 1, Fig. 2 and Supporting Information Fig. S36), we identified two compounds, **9** and **10**, presenting significant prodrug activation effects. Low doses of CAP treatment with negligible cytotoxicity were demonstrated to significantly

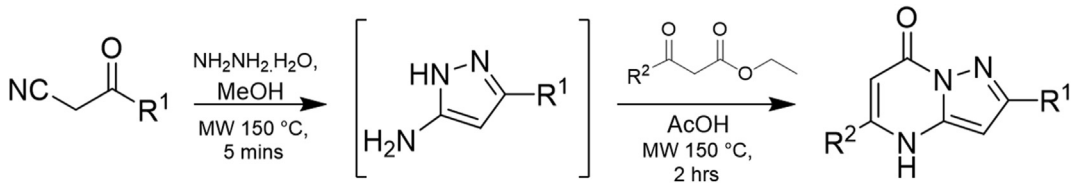

Fig. 5. Two-step synthesis of pyrazolopyrimidinones.

enhance the cytotoxic effect of **9** and **10** by more than 15 and 5 times, respectively (Fig. 2 and Table 1). The pyrazolopyrimidinone derivatives were then determined to be activated within media solution by CAP-generated ROS in culture media, which can be used to develop a prodrug strategy combined with CAP treatment. The CAP treatment can be readily targeted on the tumour site and locally activate the prodrug, thus minimising non-tumour toxicity and inducing specific therapeutic effects, especially when prodrugs have low toxicity in inactive forms. Therefore, compounds **9** and **10** can be potential core scaffold candidates for developing more sensitive and efficient prodrug derivatives.

Due to the diversity of CAP commercial devices and prototype systems, the CAP-induced ROS levels in targeted liquids and gases can vary. In our previous work, with identical conditions, 30 s of treatment performed by the same DBD CAP prototype device, targeting culture media, was shown to induce low amounts of hydrogen peroxide (H_2O_2) (~20 μM), nitrite (NO^-_2) (~5 μM), and nitrate (NO^-_3) (~30 μM) within culture media, measured by $TiSO_4$ assay, Griess reagent and 2,6-dimethylphenol assay, which are significantly less than the IC_{50} values measured previously for U-251MG cells (315 μM, >1200 μM and >600 μM respectively) [55,56]. Although many short-lived reactive species and some long-lived reactive species were not be able to be characterised, one can inference that the total amount of CAP-induced reactive species would be not major, based on the negligible cytotoxicity (Fig. 1C). On the other hand, glioblastoma cells were demonstrated to have higher ROS resistance compared to other malignant and non-malignant cells, which is considered to play major roles in the therapy resistance of glioblastoma [19,57–59]. In our previous work, using the same CAP prototype, the IC_{50} value was determined to be 4.8 s (95 % confidence range of 4.2–5.6 s) for HeLa cells and 74.26 s (95 % confidence range of 47.24–116.8 s) for U-251MG cells [19]. Non-malignant cells are usually considered to have lower level of ROS at natural status, thus their antioxidative capacity is abundant to bear higher levels of ROS [2]. In agreement to this conclusion, using the same system, 50 s of CAP treatment only decreased around 25 % viability of HEK293 cells in our another work [60]. Although, the cytotoxic effect of **10** is determined to be non-specific to tumour cells and even is slightly more cytotoxic to HEK293 cells (Supporting Information Fig. S36), the limited diffusion of reactive species from the targeted site will limit the exposure of healthy tissues to the CAP treatment, which will contribute more specific cancer cells-killing effects, in addition with targeted drug delivery strategies.

Taken together, the low doses of CAP treatment applied in this study is sufficient to generate moderate ROS levels in culture media and cells, which may activate the prodrugs and can be detected by analytical methods [61] and H_2DCFDA assay (Fig. 1A and B), respectively. The influx of extracellular ROS into the cells is considered as a main challenge of CAP treatment and is not fully understood [62]. However, in this study, due to that the cells and media were treated together between two electrodes of the DBD CAP system, the intracellular ROS may be generated directly in the liquid phase of cytoplasm, which can be detected by H_2DCFDA [63]. The limited lipid peroxidation-induced cellular responses may also contribute to the influx of extracellular ROS in this case [61].

As seen in Fig. 4, to distinguish the effects induced by CAP to cells and compounds, we have investigated the cytotoxicity of CAP-treated compounds without the direct and immediate effects caused by CAP treatment to cells. **10** was treated by CAP in DMSO solution, but demonstrated no significant enhanced cytotoxicity (Fig. 4A). 100 % DMSO contains no H_2O, which impacts on the generation of ROS [55]. Moreover, DMSO has been demonstrated to be a scavenger of OH radicals [30], together, this explains the absence of enhanced cytotoxicity of **10** in a DMSO solution without substrate. Compound **10** was then first diluted in DMEM culture medium to corresponding concentrations, and subsequently exposed to CAP treatment before being incubated with cells. Significantly enhanced cytotoxicity were observed with **10** treated by CAP in culture medium solution (Fig. 4B and C and Table 3). On the other hand, NAC has been commonly used as ROS scavenger [64], and we have found that the enhanced cytotoxicity of CAP-treated **10** in culture medium was significantly inhibited in culture medium containing NAC (Fig. 4B). Although NAC only partially recovered the cell viability, this may be due to the instant activation of **10** when ROS was generated in media or insufficient scavenger ability of NAC against some specific short-lived reactive species generated by CAP.

Recently, CAP-activated liquids, including water, PBS, saline and culture media, etc., have been explored for antimicrobial and anticancer applications [56]. Although reactive species in liquid can react to generate secondary products post-discharge, such as reactions between nitrites and hydrogen peroxide can result in peroxynitrite/peroxynitrous acid [65–67], it has been demonstrated that H_2O_2, NO^-_2 and NO^-_3 or other reactive species generated depending on the liquids or CAP systems can retain along with their antimicrobial activities for up to 7 days [55,68] and even longer term at lower temperatures [67]. In addition, Yan, D. et al. Reported that short-lived reactive species are removed by overnight storage, and most of the long-lived reactive species, such as hydrogen peroxides in the CAP-activated medium remain [69]. Mohades, S., et al. also demonstrated that CAP-activated media stored at room temperature for up to 8 h still kills around 50 % cancer cells [70].

Therefore, CAP-activated media stored overnight at 4 °C was used to test the possible activation effect towards prodrug **10.** We can determine that any oxidised component in the CAP-activated medium has no effect on the cytotoxicity of prodrug **10** and short-lived reactive species may make the main contribution to the activation of the prodrug (Supporting Information Fig. S37b). On the other hand, CAP has been found to activate various cellular responses, such as lipid peroxidation [61], accelerated cellular uptake [21,71], oxidation of protein/DNA/RNA [42], alteration of intercellular ROS signalling pathways [72], and restoring of cellular sensitivity to chemotherapy [26]. We incubated CAP-activated U-251 MG cells with **10**, therefore isolating the compounds from ROS, but observed no significant enhanced cytotoxicity or sensitivity-restoring effect (Supporting Information Fig. S37c), which demonstrated that the enhanced cytotoxicity is mainly from CAP-activated prodrug-like effect rather than CAP-activated cells. In addition, it is interesting that ROS generator, AAPH, was demonstrated to

decrease 50 % cell viability when combined with low concentrations of **10**, compared to 20 % alone, presenting a likely prodrug activation effect via generation of peroxyl radicals (ROO•) in culture medium. Moreover, only sufficient generation of peroxyl radicals would induce enhanced cytotoxicity of **10**, comparing incubation with 3 mM and 0.5 mM of AAPH (Supporting Information Fig. S36). Although, the use of ROS generator, AAPH, added to understanding activation mechanism of **10**, the potential interaction between peroxyl radicals and the prodrug-like derivatives, and their effects at higher concentration, are awaiting further exploration.

In conclusion, in this study, we tested the effect of 15 pyrozolopyrimidione derivatives on glioblastoma cell line, and four compounds (**1, 2, 4, 13**) showed IC_{50} values below 50 μM and others presented low or marginal cytotoxic activity when applied alone. Interestingly, two compounds, **9** and **10**, were discovered to possess prodrug-like effect that activated by low doses of CAP treatment. The IC_{50} values of **9** and **10** against U-251MG cells decreased from around 940 to 62 μM, and 290 to 56 μM, respectively, when combined with 30 s of CAP treatment. The CAP-generated ROS in media was then determined to play the key role in the prodrug activation process. The detailed activation mechanisms and active forms of compounds **10** and **9** is yet explored but will be investigated in future studies. This study provides potential ROS-activatable pyrazolopyrimidinone core scaffolds which contribute to the development of a CAP/ROS-trigger prodrug research that are locally activated in the tumour with minimal side effects to other tissues.

Author contributions

Z.H., P·C., J.S., and J.C. conceived the project and designed the experiments. Z.H., C·C., R.D., M.K., J.W., G.C., S.G., and J.M. performed the experiments, collected and analysed the data. Z.H., J.S., J.C., F.T., B.T., G.K., R.M., D.O., M.D. and W.W. discussed the results and co-wrote and reviewed the manuscript.

Funding

This work is supported by Irish Research Council Government of Ireland Postdoctoral Fellowship Award GOIPD/2020/788 (Z.H., J.C.) and IRCSET EMBARK grant (G.E.C., J.C.); Science Foundation Ireland Grant Numbers 14/IA/2626 (P·C., J.C.) and 17/CDA/4653 (B T., P·C., J.C.); and by the TU Dublin Fiosraigh Scholarship Programme (S·B., J.M., J.C.); Science Foundation Ireland infrastructure grants 16/RI/3399 and 12/RI/2346/SOF; Maynooth University John Hume Scholarship (M.K.); Government of Ireland Postgraduate Scholarship from the Irish Research Council (R. D.); Maynooth University Teaching Studentship (C·C.).

Declaration of competing interest

The authors declare that they have no known competing financial interests or personal relationships that could have appeared to influence the work reported in this paper.

Appendix A. Supplementary data

Supplementary data to this article can be found online at https://doi.org/10.1016/j.ejmech.2021.113736.

References

[1] H.R. Metelmann, et al., Head and neck cancer treatment and physical plasma, Clin. Plasma Med. 3 (2015) 17–23.
[2] T. von Woedtke, S. Reuter, K. Masur, K.D. Weltmann, Plasmas for medicine, Phys. Rep. 530 (2013) 291–320.
[3] X. Peng, V. Gandhi, ROS-activated anticancer prodrugs: a new strategy for tumor-specific damage, Ther. Deliv. 3 (2012) 823–833.
[4] C. Welz, et al., Cold atmospheric plasma: a promising complementary therapy for squamous head and neck cancer, PloS One 10 (2015) 1–15.
[5] M. Görmen, et al., Synthesis, cytotoxicity, and COMPARE analysis of ferrocene and [3]ferrocenophane tetrasubstituted olefin derivatives against human cancer cells, ChemMedChem 5 (2010) 2039–2050.
[6] H. Lin, et al., Pyrazolopyrimidine derivatives as PI3 kinase inhibitors, WO Pat WO2013028263 (2013).
[7] B. Gu, T. Block, A. Cuconati, Small molecule inhibitors against west nile virus replication, *WO Pat* WO2007005541, 2007.
[8] S. Cherukupalli, et al., An insight on synthetic and medicinal aspects of pyrazolo[1,5-a]pyrimidine scaffold, Eur. J. Med. Chem. (2017) 126 298–352.
[9] D.A. Griffith, et al., Discovery and evaluation of pyrazolo[1,5-a]pyrimidines as neuropeptide Y1 receptor antagonists, Bioorg. Med. Chem. Lett 21 (2011) 2641–2645.
[10] W. McCoull, et al., Identification of pyrazolo-pyrimidinones as GHS-R1a antagonists and inverse agonists for the treatment of obesity, Medchemcomm 4 (2013) 456–462.
[11] M. Kelada, J.M.D. Walsh, R.W. Devine, P. McArdle, J.C. Stephens, Synthesis of pyrazolopyrimidinones using a “one-pot” approach under microwave irradiation, Beilstein J. Org. Chem. 14 (2018) 122–1228.
[12] H. Binch, L. Fanning, Modulators of cystic fibrosis transmembrane conductance regulator, Google Patents (2012). www.genet.sickkids.on.ca/cftr/.
[13] A.M. Venkatesan, et al., Novel imidazolopyrimidines as dual PI3-Kinase/mTOR inhibitors, Bioorg. Med. Chem. Lett 20 (2010) 653–656.
[14] A.J. Folkes, et al., The identification of 2-(1H-indazol-4-yl)-6-(4-methanesulfonyl-piperazin-1- ylmethyl)-4-morpholin-4-yl-thieno[3,2-d]pyrimidine (GDC-0941) as a potent, selective, orally bioavailable inhibitor of class I PI3 kinase for the treatment of cancer, J. Med. Chem. 51 (2008) 5522–5532.
[15] A.J. Peat, et al., Novel pyrazolopyrimidine derivatives as GSK-3 inhibitors, Bioorg. Med. Chem. Lett 14 (2004) 2121–2125.
[16] S. Martina Ferrari, et al., Pyrazolopyrimidine derivatives as antineoplastic agents: with a special focus on thyroid cancer, Mini Rev. Med. Chem. 16 (2015) 86–93.
[17] J. O'donnell-Tormey, C.F. Nathan, K. Lanks, C.J. Deboer, J. De La Harpe, Secretion of pyruvate: an antioxidant defense of mammalian cells, J. Exp. Med. 165 (1987) 500–514.
[18] T. Moiseev, et al., Post-discharge gas composition of a large-gap DBD in humid air by UV-Vis absorption spectroscopy, Plasma Sources Sci. Technol. 23 (2014).
[19] G.E. Conway, et al., Non-thermal atmospheric plasma induces ROS-independent cell death in U373MG glioma cells and augments the cytotoxicity of temozolomide, Br. J. Canc. 114 (2016) 435–443.
[20] T.C. Chou, N. Martin, CompuSyn for drug combinations. *A comput. Softw. Quant. Synerg. Antagon. Determ. IC50, ED50 LD50 values*, [PC Softw. user's Guid. Paramus, NJ, 2005.
[21] Z. He, et al., Cold atmospheric plasma induces ATP-dependent endocytosis of nanoparticles and synergistic U373MG cancer cell death, Sci. Rep. 8 (2018) 1–11.
[22] P. Babington, et al., Use of cold atmospheric plasma in the treatment of cancer, Biointerphases 10 (2015), 029403.
[23] F. Utsumi, et al., Effect of indirect nonequilibrium atmospheric pressure plasma on anti-proliferative activity against chronic chemo-resistant ovarian cancer cells in vitro and in vivo, PloS One 8 (2013).
[24] S. Park, et al., Cold atmospheric plasma restores paclitaxel sensitivity to paclitaxel-resistant breast cancer cells by reversing expression of resistance-related genes, Cancers 11 (2019).
[25] S. Lee, et al., Cold atmospheric plasma restores tamoxifen sensitivity in resistant MCF-7 breast cancer cell, Free Radic. Biol. Med. 110 (2017) 280–290.
[26] J. Köritzer, et al., Restoration of sensitivity in chemo - resistant glioma cells by cold atmospheric plasma, PloS One 8 (2013), e64498.
[27] H. Tamta, S. Kalra, A.K. Mukhopadhyay, Biochemical characterization of some pyrazolopyrimidine-based inhibitors of xanthine oxidase, Biochemist (2006), https://doi.org/10.1134/S0006297906130086.
[28] S. Gaonkar, et al., Novel pyrazolo[3,4-d]pyrimidine derivatives inhibit human cancer cell proliferation and induce apoptosis by ROS generation, Arch. Pharm. (Weinheim) 353 (2020) 1–13.
[29] H. Tanaka, et al., Plasma-activated medium selectively kills glioblastoma brain tumor cells by down-regulating a survival signaling molecule, AKT kinase, Plasma Med. 1 (2011) 265–277.
[30] M.K. Eberhardt, R. Colina, The reaction of OH radicals with dimethyl sulfoxide. A comparative study of fenton's reagent and the radiolysis of aqueous dimethyl sulfoxide solutions, J. Org. Chem. 53 (1988) 1071–1074.
[31] V. Barygina, et al., ROS-challenged keratinocytes as a new model for oxidative stress-mediated skin diseases, J. Cell. Biochem. 120 (2019) 28–36.
[32] R.R. He, et al., A new oxidative stress model, 2,2-azobis(2-amidinopropane) dihydrochloride induces cardiovascular damages in chicken embryo, PloS One 8 (2013).
[33] S. Oppermann, et al., High-content screening identifies kinase inhibitors that overcome venetoclax resistance in activated CLL cells, Blood 128 (2016) 934–947.
[34] L.J. Murray, M.H. Robinson, Radiotherapy: technical aspects, Med. Plus 44 (2016) 10–14.
[35] K. Tachibana, L.B. Feril, Y. Ikeda-Dantsuji, Sonodynamic therapy, Ultrasonics 48 (2008) 253–259.

[36] M.A. Calin, S.V. Parasca, Photodynamic therapy in oncology, J. Optoelectron. Adv. Mater. 8 (2006) 1173–1179.
[37] S.C. Gupta, et al., Upsides and downsides of reactive oxygen species for Cancer: the roles of reactive oxygen species in tumorigenesis, prevention, and therapy, Antioxidants Redox Signal. 16 (2012) 1295–1322.
[38] S.Y. Sun, et al., Mediation of N-(4-hydoxyphenyl)retinamide-induced apoptosis in human cancer cells by different mechanisms, Canc. Res. 59 (1999) 2493–2498.
[39] J. Gao, X. Liu, B. Rigas, Nitric oxide-donating aspirin induces apoptosis in human colon cancer cells through induction of oxidative stress, Proc. Natl. Acad. Sci. U.S.A. 102 (2005) 17207–17212.
[40] E.M. Hersh, et al., Antiproliferative and antitumor activity of the 2-cyanoaziridine compound imexon on tumor cell lines and fresh tumor cells in vitro, J. Natl. Cancer Inst. 84 (1992) 1238–1244.
[41] A.M. Evens, et al., Motexafin gadolinium generates reactive oxygen species and induces apoptosis in sensitive and highly resistant multiple myeloma cells, Blood 105 (2005) 1265–1273.
[42] C.V. Suschek, C. Opländer, The application of cold atmospheric plasma in medicine: the potential role of nitric oxide in plasma-induced effects, Clin. Plasma Med. 4 (2016) 1–8.
[43] L. Xiang, X. Xu, S. Zhang, D. Cai, X. Dai, Cold atmospheric plasma conveys selectivity on triple negative breast cancer cells both in vitro and in vivo, Free Radic. Biol. Med. 124 (2018) 205–213.
[44] D. Yan, et al., Principles of using cold atmospheric plasma stimulated media for cancer treatment, Sci. Rep. 5 (2015) 18339.
[45] C. Le Manach, et al., A novel pyrazolopyridine with in vivo activity in Plasmodium berghei- and Plasmodium falciparum-infected mouse models from structure-activity relationship studies around the core of recently identified antimalarial imidazopyridazines, J. Med. Chem. 58 (2015) 8713–8722.
[46] C. García-Echeverría, Allosteric and ATP-competitive kinase inhibitors of mTOR for cancer treatment, Bioorg. Med. Chem. Lett 20 (2010) 4308–4312.
[47] M. Chauhan, R. Kumar, Medicinal attributes of pyrazolo[3,4-d]pyrimidines: a review, Bioorg. Med. Chem. 21 (2013) 5657–5668.
[48] L. Scheppke, et al., Retinal vascular permeability suppression by topical application of a novel VEGFR2/Src kinase inhibitor in mice and rabbits, J. Clin. Invest. 118 (2008) 2337–2346.
[49] L.J. Phillipson, et al., Discovery and SAR of novel pyrazolo[1,5-a]pyrimidines as inhibitors of CDK9, Bioorg. Med. Chem. 23 (2015) 6280–6296.
[50] D.A. Heathcote, et al., A novel pyrazolo[1,5- a]pyrimidine is a potent inhibitor of cyclin-dependent protein kinases 1, 2, and 9, which demonstrates antitumor effects in human tumor xenografts following oral administration, J. Med. Chem. 53 (2010) 8508–8522.
[51] Dwyer, M., Paruch, K., Labroli, M., … C. A.-B. & medicinal & 2011, undefined. pyrimidine-based CHK1 inhibitors: A Template-Based Approach—Part 1. Elsevier.
[52] D.M. Berger, et al., Non-hinge-binding pyrazolo[1,5-a]pyrimidines as potent B-Raf kinase inhibitors, Bioorg. Med. Chem. Lett 19 (2009) 6519–6523.
[53] M.R. Shaaban, T.S. Saleh, A.S. Mayhoub, A.M. Farag, Single step synthesis of new fused pyrimidine derivatives and their evaluation as potent Aurora-A kinase inhibitors, Eur. J. Med. Chem. 46 (2011) 3690–3695.
[54] N.S.M. Ismail, G.M.E. Ali, D.A. Ibrahim, A.M. Elmetwali, Medicinal attributes of pyrazolo[1,5-a]pyrimidine based scaffold derivatives targeting kinases as anticancer agents, Futur. J. Pharm. Sci. 2 (2016) 60–70.
[55] P. Lu, D. Boehm, P. Bourke, P.J. Cullen, Achieving reactive species specificity within plasma-activated water through selective generation using air spark and glow discharges, Plasma Process. Polym. 14 (2017) 1–9.
[56] E. Tsoukou, P. Bourke, D. Boehm, Understanding the differences between antimicrobial and cytotoxic properties of plasma activated liquids, Plasma Med. 8 (2018) 299–320.
[57] C. Olivier, L. Oliver, L. Lalier, F.M. Vallette, Drug resistance in glioblastoma: the two faces of oxidative stress, Frontiers in Molecular Biosciences 7 (2021).
[58] E. Singer, et al., Reactive oxygen species-mediated therapeutic response and resistance in glioblastoma, Cell Death Dis. 6 (2015).
[59] H.C. Lee, et al., Increased expression of antioxidant enzymes in radioresistant variant from U251 human glioblastoma cell line, Int. J. Mol. Med. 13 (2004) 883–887.
[60] S. Gunes, et al., Platinum nanoparticles inhibit intracellular ROS generation and protect against Cold Atmospheric Plasma-induced cytotoxicity, biorxiv.org (2021), https://doi.org/10.1101/2021.02.18.431888.
[61] Z. He, et al., Cold atmospheric plasma stimulates clathrin-dependent endocytosis to repair oxidised membrane and enhance uptake of nanomaterial in glioblastoma multiforme cells, Sci. Rep. 10 (2020).
[62] R. Moniruzzaman, et al., Roles of intracellular and extracellular ROS formation in apoptosis induced by cold atmospheric helium plasma and X-irradiation in the presence of sulfasalazine, Free Radic. Biol. Med. 129 (2018) 537–547.
[63] G.E. Conway, et al., Cold Atmospheric Plasma induces accumulation of lysosomes and caspase-independent cell death in U373MG glioblastoma multiforme cells, Sci. Rep. 9 (2019) 1–29.
[64] I. Downs, J. Liu, T.Y. Aw, P.A. Adegboyega, M.N. Ajuebor, The ROS scavenger, NAC, regulates hepatic Vα14iNKT cells signaling during Fas mAB-dependent fulminant liver failure, PloS One 7 (2012).
[65] P. Lukes, E. Dolezalova, I. Sisrova, M. Clupek, Aqueous-phase chemistry and bactericidal effects from an air discharge plasma in contact with water: evidence for the formation of peroxynitrite through a pseudo-second-order post-discharge reaction of H2O 2 and HNO2, Plasma Sources Sci. Technol. 23 (2014), 015019.
[66] S. Ikawa, A. Tani, Y. Nakashima, K. Kitano, Physicochemical properties of bactericidal plasma-treated water, J. Phys. D Appl. Phys. 49 (2016) 425401.
[67] E. Tsoukou, P. Bourke, D. Boehm, Temperature stability and effectiveness of plasma-activated liquids over an 18 months period, Water 12 (2020) 1–18.
[68] M.J. Traylor, et al., Long-term antibacterial efficacy of air plasma-activated water, J. Phys. D Appl. Phys. 44 (2011).
[69] D. Yan, et al., Stabilizing the cold plasma-stimulated medium by regulating medium's composition, Sci. Rep. 6 (2016).
[70] S. Mohades, M. Laroussi, J. Sears, N. Barekzi, H. Razavi, Evaluation of the effects of a plasma activated medium on cancer cells, Phys. Plasmas 22 (2015).
[71] X. Cheng, et al., Synergistic effect of gold nanoparticles and cold plasma on glioblastoma cancer therapy, J. Phys. D Appl. Phys. 47 (2014) 335402.
[72] E. Stoffels, Y. Sakiyama, D.B. Graves, Cold atmospheric plasma: charged species and their interactions with cells and tissues, IEEE Trans. Plasma Sci. 36 (2008) 1441–1457.